Biotechnol. J. 2009, 4, 903–913 DOI 10.1002/biot.200900007 www.biotechnology-journal.com

Research Article

Automated classification of *Plasmodium* sporozoite movement patterns reveals a shift towards productive motility during salivary gland infection

Stephan Hegge, Mikhail Kudryashev*, Ashley Smith and Friedrich Frischknecht*

Department of Parasitology, Hygiene Institute, University of Heidelberg Medical School, Heidelberg, Germany

The invasive stages of malaria and other apicomplexan parasites use a unique motility machinery based on actin, myosin and a number of parasite-specific proteins to invade host cells and tissues. The crucial importance of this motility machinery at several stages of the life cycle of these parasites makes the individual components potential drug targets. The different stages of the malaria parasite exhibit strikingly diverse movement patterns, likely reflecting the varied needs to achieve successful invasion. Here, we describe a Tool for Automated Sporozoite Tracking (ToAST) that allows the rapid simultaneous analysis of several hundred motile *Plasmodium* sporozoites, the stage of the malaria parasite transmitted by the mosquito. ToAST reliably categorizes different modes of sporozoite movement and can be used for both tracking changes in movement patterns and comparing overall movement parameters, such as average speed or the persistence of sporozoites undergoing a certain type of movement. This allows the comparison of potentially small differences between distinct parasite populations and will enable screening of drug libraries to find inhibitors of sporozoite motility. Using ToAST, we find that isolated sporozoites change their movement patterns towards productive motility during the first week after infection of mosquito salivary glands.

Received 13 January 2009
Revised 5 March 2009
Accepted 3 April 2009

Keywords: Gliding motility · Malaria · Object tracking · *Plasmodium* sporozoite

1 Introduction

Pathogens often rely on their own motility (*e.g.* bacterial flagellar motion) to enter host organisms and cells [1–6]. In the case of malaria, the *Plasmodium* parasite relies on a motility apparatus at different stages of the life cycle that is based on an actin-myosin motor and the retrograde capping of secreted surface adhesins [7–9]. *Plasmodium* merozoites bind to red blood cells and enter them actively by means of this motor before replicating within the cell [10]. Within the mosquito gut, motile ookinetes can penetrate the epithelium. Like merozoites, ookinetes rely on the actin-myosin motor to move, but they do not invade an epithelial cell to remain intracellular. Instead, ookinetes migrate through epithelial cells and form a cyst at the basal side of the epithelium [11]. Within this cyst, *Plasmodium* sporozoites develop and eventually enter the salivary glands to be transmitted back to the host during a mosquito bite [12]. Similar to other arthropod-borne disease agents, the majority of sporozoites are injected into the skin, while a few might directly enter the bloodstream [13–20]. While sporozoites within the salivary gland rarely move, those transmitted into the skin move at high speed

Correspondence: Friedrich Frischknecht, Department of Parasitology, Hygiene Institute, University of Heidelberg Medical School, Im Neuenheimer Feld 324, 69120 Heidelberg, Germany
E-mail: freddy.frischknecht@med.uni-heidelberg.de
Fax: +49-6221-564643

Abbreviations: CW, clockwise; **CCW**, counter-clockwise; **ToAST**, tool for automated sporozoite tracking

*The first two authors contributed equally to this work.

[14, 21, 22]. Some of these transmitted sporozoites actively enter blood vessels and penetrate the liver parenchyma, where they eventually invade hepatocytes to multiply into thousands of merozoites [23]. Clearly, to inhibit sporozoite motility means to interrupt transmission of the disease, as the parasite is not able to reach and invade hepatocytes [12, 24].

Plasmodium sporozoites also move *in vitro* [25, 26]. Sporozoites isolated from infected salivary glands can undergo attached waving, a movement not associated with translocation, where the parasite is attached with one end and waves with its body in the medium [26]. Little is known about the molecular base of this movement. Alternatively, these sporozoites can undergo actin- and myosin-dependent gliding motility, whereby they translocate without changing their shape [7, 25, 26]. Sporozoites are highly polarized and crescent-shaped cells, which glide with their apical (front) end leading. *In vitro* sporozoites move in circles with one preferred direction [26]. This makes them amenable for visual analysis like almost no other cell, as it allows long-term observation of single parasites moving for up to dozens of minutes without leaving the field of view. Here, we developed a tracking tool that allows the classification of movement patterns and other parameters describing sporozoite motion. This tool will also enable us to conduct a high-throughput search for inhibitors targeting the gliding motility machinery.

2 Materials and methods

2.1 Parasites and microscopy

Plasmodium berghei (strain NK65) sporozoites expressing green fluorescent protein (GFP) [27] were produced in *Anopheles stephensi* mosquitoes essentially as described previously [21]. Salivary glands were dissected and sporozoites isolated in a 1.5-mL reaction tube containing RPMI tissue culture medium with 3% bovine serum albumin. For imaging, sporozoites were placed in a well of a 384-well plate (flat-bottom, black with 0.9-mm clear polystyrene bottom; Corning, Wiesbaden, Germany). The plates were centrifuged (room temperature, 200 × g, 3 min) and imaging was performed on an inverted Axiovert 200M Zeiss microscope in an air-conditioned imaging suite at room temperature (24°C) or at 37°C in a heated incubator (part of the Zeiss CellObserver system). Images were collected with a Zeiss Axiocam HRm every 1 or 2 s using Axiovision 4.6 software and various objective lenses (10× Apoplan objective, NA 0.25; 63× Plan-Apochromat, NA 1.40). All image series were eventually imported to ImageJ for analysis and figures were generated using the Adobe Creative Suite software package.

2.2 Image processing

2.2.1 Global thresholding for signal detection

For each frame in a time-lapse image series, the mean (M) pixel value and average deviation from the mean (AD) were calculated and the global threshold of M + *n*AD was applied for each picture separately (this was implemented as 'the Thresholder plugin') with typical values for $n = 5, 7, 9$. Pictures were processed separately as the overall intensity may have decreased over the time of acquisition due to photobleaching. Adjacent pixels were segmented into one object.

2.2.2 Automatic sporozoite tracking

Particle tracking was essentially performed with the MTrack2 plugin implemented by Nico Stuurman (http://valelab.ucsf.edu/~nico/IJplugins/MTrack2.html). It identifies the objects in each frame of a thresholded movie and determines which objects in the successive frames are closest together. If these are located within a user-defined distance limit, then these objects are assembled to a track. In order to distinguish sporozoites from mosquito salivary gland tissue debris that occasionally may be present in the movies, we introduced a spherical factor (SPF) of an object as a correlation coefficient between x and y coordinates of all object pixels in a coordinate system tilted 45° to the principal axis of the object. The SPF varies from 0 for a round object to 1 for an ideal line and is typically 0.75–0.9 for a sporozoite. For our analysis, all objects with an average SPF below 0.4 for the whole track length were removed from the resulting log-file.

2.2.3 Classification of sporozoite motility patterns

The translational speed v and the angle increment α for each time point for each parasite was calculated from the coordinates, pixel size and time interval between frames. Next, averaging over $2k + 1$ (k is the sliding average half-size, a user-defined parameter with a typical value of 4 for 0.5-Hz image series) consecutive time points for every track was performed. The averaging reduced the noise present in a low-magnification image series and thus yielded more reliable values for v and α. All objects with an average speed $v \leq 0.5$ µm/s were assigned as "attached" parasites. All objects having an average *absolute* value of $\alpha \leq v/45$ were assigned as gliders; all the others were assigned as wavers, with

45 corresponding to the angle of the separation line between gliders and wavers. This number was empirically determined to minimize the error in automated *versus* manual annotation. Then, gliders were sub-classified into either counter-clockwise (CCW) gliding, which is gliding with a negative average angle increment, or clockwise (CW) gliding (positive average angle increment). The steps described under 2.2.2 and 2.2.3 were implemented into our ImageJ plugin 'ToAST' (Tool for Automated Sporozoite Tracking), which is part of the ImageJ based open source processing package Fiji.

2.2.4 Processing of multiple movie files

Processing of multiple image series was performed by an ImageJ macro in the following steps: Movie files with consistent filenames were loaded, (semi)automatically thresholded by the 'thresholder plugin' (user has to set the number of average deviations based on the quality of the signal) and processed *via* 'ToAST'. The resulting tracking output of every movie was stored in a text file, together with the thresholded and tracked movies and a tiff-image showing the paths of all assigned tracks. The original files remain unmodified. The data visualization was accomplished with a Microsoft Excel macro.

2.3 Error estimation

"Easy-to-classify parasites" that followed the same motility pattern over the whole duration of observation were first manually assigned to the motility states in the following way: The percentage of gliding, waving and being attached was assigned for every parasite. The overall percentage for six parasites showing simple motility patterns was compared to the results of the corresponding automatic assignment.

"Difficult-to-classify parasites" that frequently changed their motility patterns were assigned to the motility states frame by frame by several non-experienced and experienced users asked to memorize only the three previous time frames. Then, for every time point a consensus assignment was made if most of the users agreed on one of the states; otherwise the respective time points remained unannotated. Finally, manual assignment was compared to the automatic annotation.

3 Results

3.1 Distinct sporozoite movement patterns

To visualize moving *Plasmodium* sporozoites, we isolated parasites expressing cytoplasmic GFP from mosquito salivary glands. Imaging was performed with a variety of frame rates on a wide-field fluorescence microscope with either 10× or 63× objective lenses (pixel size: 627×627 and 98×98 nm^2, respectively). High-magnification imaging readily revealed the different movement patterns: (i) drifting, which describes parasites not yet adherent on the substrate; (ii) attached, which describes sporozoites adherent with one end and the other end showing only small displacements; (iii) waving, which describes parasites attached with one end to the substrate and the other end moving actively in the medium; (iv) gliding in a CCW direction and (v) gliding in a CW direction (Fig. 1). These distinct parasite movement patterns could also be reliably observed with a 10× objective, allowing simultaneous tracking up to 250 sporozoites (Fig. 2A–C). Thresholding of the fluorescent signal and maximum fluorescent intensity projections allowed the visualization of movement patterns and formed the basis for quantitative analysis. Projections of movies over only 20 frames recorded at 1 Hz showed mainly homogenous patterns of movements (Fig. 2D, white projections), while projections over longer periods of time (Fig. 2D, red projections) revealed that parasites did not just undergo one type of movement, but could switch between different movements (Fig. 2D, E) as originally reported [26].

3.2 Tracking motile parasites

As drifting does not describe an active movement of the parasites and we anticipated problems of differentiating between this and other types of movement, we centrifuged the parasites at $200 \times g$ for 3 min, which abrogated drifting while the other movement patterns were still observed. To determine the speed of sporozoites, we compared the results of different manual approaches using the manual tracking tool of ImageJ (Mtrack) to those derived by the automatic Mtrack2 plugin. We tracked the same sporozoites acquired at 100× with 0.5 Hz in four different ways: (1) manual tracking of the front end of the sporozoite one time each by three different users (Fig. 3B, 1t 3p); (2) manual tracking of the front end of the sporozoite by the same user repeated three times (Fig. 3B, 3t 1p); (3) manual tracking of the center of the sporozoite by one user repeated three times (Fig. 3B, 3t 1p);

Biotechnol. J. 2009, 4, 903–913

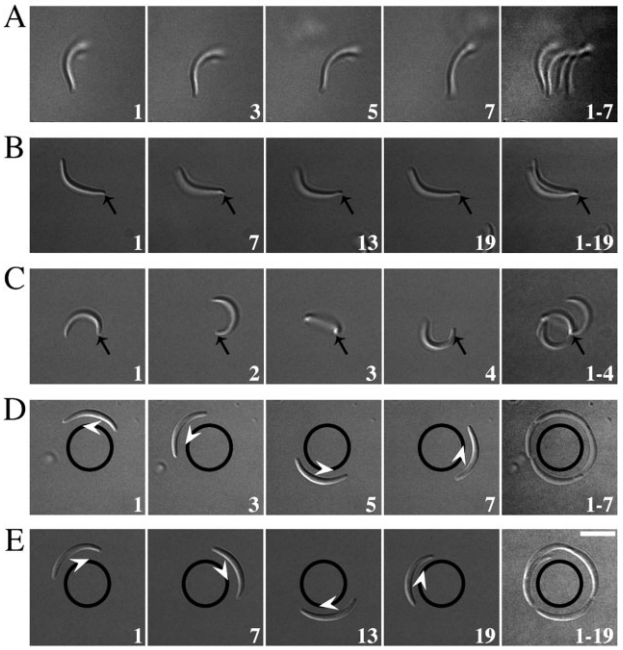

Figure 1. Different movement patterns of sporozoites. The right pictures represent the sum of the differential interference contrast (DIC) images from the previous time points in each row. Numbers indicate time in seconds. Imaging was performed with a 63× objective, scale bar: 5 μm. (A) Drifting. Sporozoites float passively in the medium. (B) Attached. Sporozoites float with one end while the other end (arrow) is attached to the substrate. (C) Waving. Sporozoites are with one end attached to the substrate (arrow) while the other end is actively moving. (D, E) Gliding. Sporozoites glide in circles either CCW (D) or CW (E).

(4) automated tracking of the sporozoite's center (Mtrack2) with different threshold values, namely 3, 5 and 7 average deviations using the 'automatic thresholder' plugin (Fig. 3B, 3thr Mac). All four approaches showed differences in speed from one measurement of the same frame to another. However, the lowest standard deviation was observed for automated tracking, which also resulted in the lowest average speed (Fig. 3B). This apparent decrease in speed is due to waving behaviors between gliding intervals as a waving sporozoite shows smaller displacements at the center than at the tip. In perfectly circular gliding sporozoites, no difference in average speed is detected (data not shown). Intuitively, imaging at low frequency decreases the speed of the circular moving parasites (Fig. 3C). However, an increase in sampling rate will not indefinitely improve the measurement, as at high frame rates the tracking error will eventually cause an artificial increase in the tracked distance covered by a moving object (Fig. 3D and S. Münter, M. Kudryashev, S. Hegge and F. Frischknecht, unpublished data).

3.3 Automated classification of movement patterns

In order to test the possibility of distinguishing between the different patterns of movement, including those that do not contribute to active locomotion, we investigated 100 consecutive frames imaged at 1 Hz and manually assigned sporozoites showing either simple or more complex linear combinations of the described patterns (Fig. 3E). The variability of manual tracking was assessed by different users. Persons who had never classified parasites before, termed inexperienced users, as well as experienced users who had regularly tracked and classified sporozoites previously were asked to assign one of the four different movement features to the same set of parasites. Subsequently, the agreement between these two groups of users was measured by the number of identically assigned frames (Fig. 3F). This yielded a larger observer error than simple tracking of gliding sporozoites. As expected, classifying 'easy-to-classify' parasites yielded the highest agreement between all sets of users and served as a control. More difficult patterns of movement, namely when a sporozoite switched the type of movement several times, resulted in a lower overall agreement, although experienced users had a higher agreement than inexperienced users. Surprisingly, waving parasites never showed matches better than 60%. Analysis of the raw data revealed that human judgment varies the most when trying to distinguish between passive motion of a sporozoite, which then would be mistakenly assigned as 'attached', and slow active motion, which then would be assigned as 'waving'. This error between observers was particularly apparent when parasites underwent frequent changes between movement patterns (*e.g.* gliding CW followed by waving followed by gliding CCW *etc.*).

In order to computationally distinguish between these patterns, we calculated the translational speed v as the distance between the center of the same parasite in two consecutive frames and the relative angle increment α between the directions of two consecutive displacement moves of a parasite (Fig. 4A) and plotted one against the other (Fig. 4B). Parasites undergoing gliding motility were characterized by high speed which, on average, related linearly to the absolute value of rotational speed for every single sporozoite. Next, sporozoites gliding CW could be distinguished from those gliding CCW when the exact value and the sign of α was plotted against the translational speed (Fig. 4C–E). Parasites that were attached showed little displacement at very low speed, while those undergoing waving motion underwent a

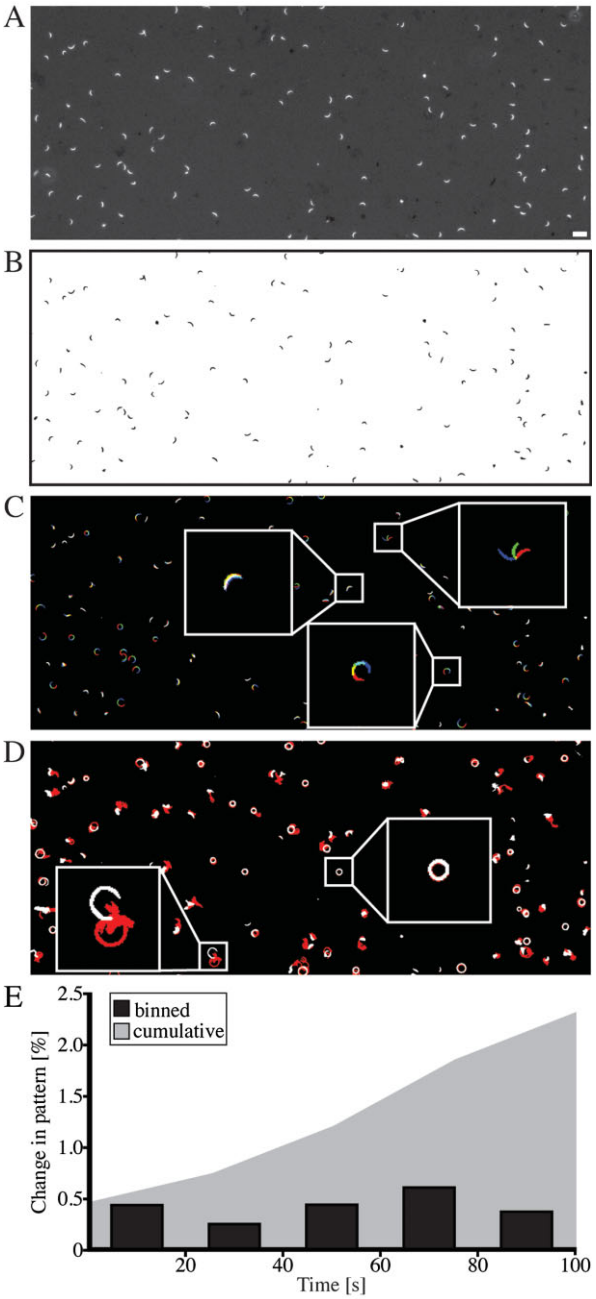

Figure 2. Detection of movement patterns from low-magnification movies. (A) One half of a microscopic image of salivary gland sporozoites expressing GFP recorded with a 10× objective. (B) Thresholded and inverted image showing signal (black) and background (white) in a 1-bit image produced from (A) using the automatic thresholder plugin (5 AD). (C) Color-coded overlay of three thresholded images recorded 4 s apart. Colors indicate different time points (blue 0 s, green 4 s, red 8 s). Insets highlight three different types of movement: attached (left), waving (right) and gliding CCW (middle). (D) Maximum intensity projections of 20 s (white) and 100 s (red). Some sporozoites show robust gliding (right inset), while others switch between patterns over time (left inset). (E) Sporozoites changing movement pattern over time. The percentage of sporozoites changing their pattern of movement over a 20-s period is constantly below 1%. 108 parasites were observed for 100 s from one movie (1 frame per second, 10 800 data points).

range of angular displacements at an intermediary speed (Fig. 4B). In order to reduce the noise from automated tracking, we employed averaging of translational and rotational speeds over $2k + 1$ time frames (Fig. 4B). For our imaging conditions, we set k to be 4–8. Finally, in order to quantify the number of different states of movement in a population over the time of observation, we counted the number of points in each area (Fig. 4B). Examination of parasites that showed a range of different movements revealed that this way of distinguishing between patterns provided only a rough estimate, and relied on a manual setting of the borders that delineated the data points into a particular category. However, as the attached parasites resulted in a cloud of points that always fell in the range below 0.5 µm/s, we delineated attached sporozoites from the others at this speed (Fig. 4B). Sporozoites moving in circles showed a correlation between v and α of about 0.95, which made the dependence in the scatter for every single track close to linear. Maximal observed angles of inclination of the v/α line never exceeded 0.02 µm/(s × degree), which made it possible to computationally isolate gliding parasites. Waving sporozoites showed high variation in both translational and rotational speeds and thus were the hardest to classify both manually and computationally. The whole procedure from loading the stored movies till visualization of the result windows in Excel was called a Tool for Automated Sporozoite Tracking (ToAST) (Fig. 4F, G).

3.4 Automated *versus* manual assignment of movement types

Comparison of automated classification with user-based assignments for "difficult-to-classify" parasites revealed a better agreement for the identification of attached and motile states than for wavers by both inexperienced and experienced users (Fig. 5A). As expected, experienced users had a higher match to the automated procedure results. Still, the overall reliability of classification of parasites exhibiting complex movement patterns was low.

However, these difficult-to-classify sporozoites constitute only a small minority of the imaged population (≤5%, see Fig. 2D). Therefore, comparing the automated classification (automatic thresholding applying 5, 7 and 9 average deviations) to the annotation by three experienced users for an entire movie (100 frames at 1 Hz) containing over 100 sporozoites showed that the overall classification is highly reliable (Fig. 5B). Less reliability might be observed when ToAST is applied on other parasites

Biotechnol. J. 2009, 4, 903–913

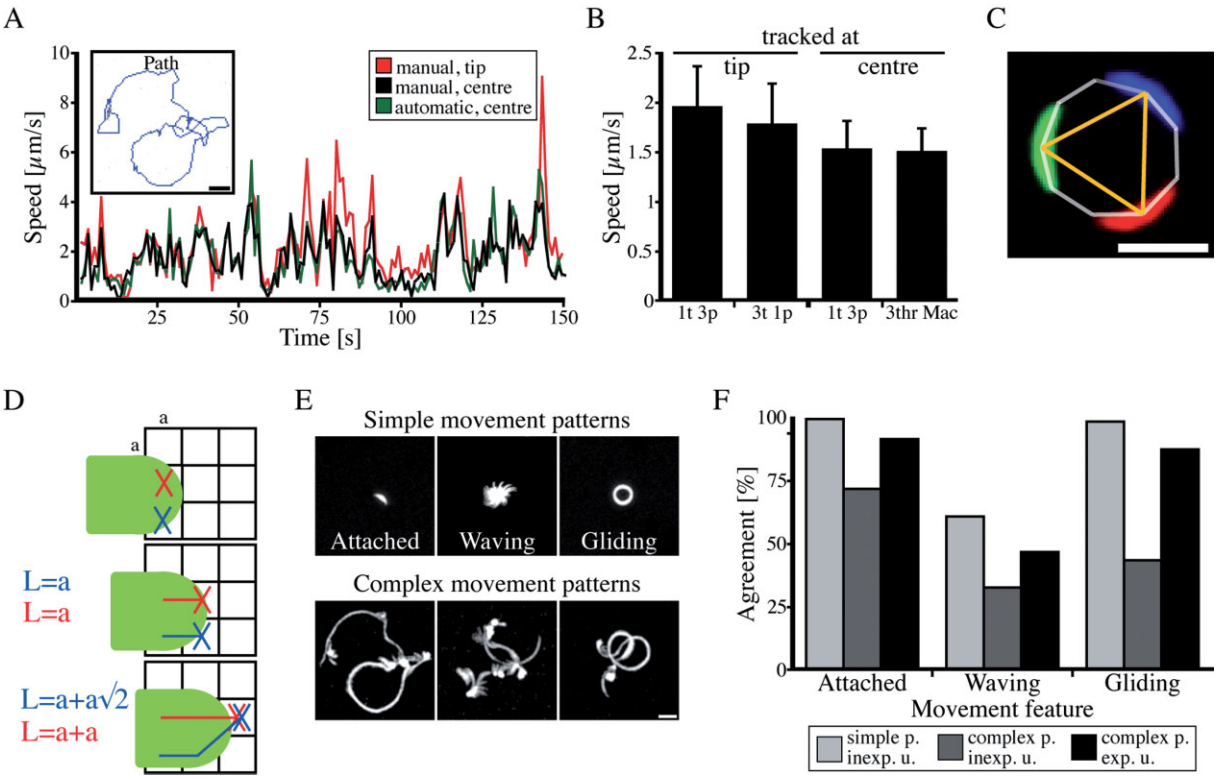

Figure 3. Reliability of manual and automated tracking of sporozoite motility. (A) Speed for a single parasite tracked three times either manually or automatically. Speeds derived from manual tracking at the parasites tip (red) or center (black) by three persons and automatic tracking at the center (green) with three different threshold levels: mean + *n*AD, *n* = 5, 7, 9. Inset shows the tracked sporozoite path. Scale bar = 10 μm. (B) Median speeds and average standard deviations of a single sporozoite tracked either at the tip manually by three persons once (tip, 1t 3p), by one person three times (tip, 3t 1p), at the center by three persons once (centre, 1t 3p) or automatically with three different thresholds (centre, 3thr Mac). (C, D) Sources of tracking errors by under-sampling (C) and over-sampling (D). (C) Scheme representing a CCW gliding sporozoite at three time points (blue, green, red). Tracking leads to shorter distances over a given amount of time when images were taken every 9 s (yellow line, under-sampling) compared to every 3 s (white line). (D) A scheme illustrating one possible source of tracking error from images taken at high temporal resolution. The tip of an object (green) can be tracked either by the red or the blue cross. The paths differ in distance. This distance, *i.e.* the potential tracking error, will increase with the number of images taken between time points (over-sampling). (E) Maximum intensity projections (100 frames at 1 Hz) of different motility patterns as imaged through a 10× objective. The upper panel shows the three simple patterns of 'attached', 'waving' and 'gliding' parasites; the lower panel displays more complex patterns consisting of linear combinations of the three simple patterns. Scale bar = 10 μm. (F) Results of manual assignments of the movement patterns in (E). The agreement between two individuals differs between inexperienced and experienced users (inexp. and exp. u.) and between simple and complex movement patterns (simple and complex p.). Simple patterns show the strongest agreement and have a low variation between both user groups (bright bars and data not shown). The agreement when classifying complex patterns drops for both user groups (dark and black bars) when comparing to simple patterns, though experienced users perform better for all movement features (black bars). Waving shows the lowest values and never exceeds 60% agreement between two users. The dataset with simple (difficult) movement patterns contained 5 (7) sporozoites and 900 (1018) data points. Each track was assigned to one of the motility states by 2.6 inexperienced and 5 experienced users.

such as *Toxoplasma gondii* tachyzoites, which change movement patterns more frequently.

3.5 ToAST reveals a shift of movement patterns during sporozoite maturation

We applied ToAST to test a number of different sporozoite preparations derived from infected mosquitoes at different days after the mosquitoes received their infective blood meal. First, we tested whether sporozoites from mosquitoes dissected at the same time show different movement patterns and average speeds if separated in classes of 'low-level' and 'high-level' salivary gland infection. We found no difference in any of the tested movement parameters, including overall sporozoite speed (Fig. 6A, B). When sporozoites were imaged at room temperature or at 37°C, the percentage of productive gliders dropped faster at higher temperature (Fig. 6C). Gliding sporozoites moved consistently faster at higher temperature, but the speed of those moving at room temperature remained constant over a longer time (Fig. 6D). As sporozoites are thought to mature within the salivary glands and

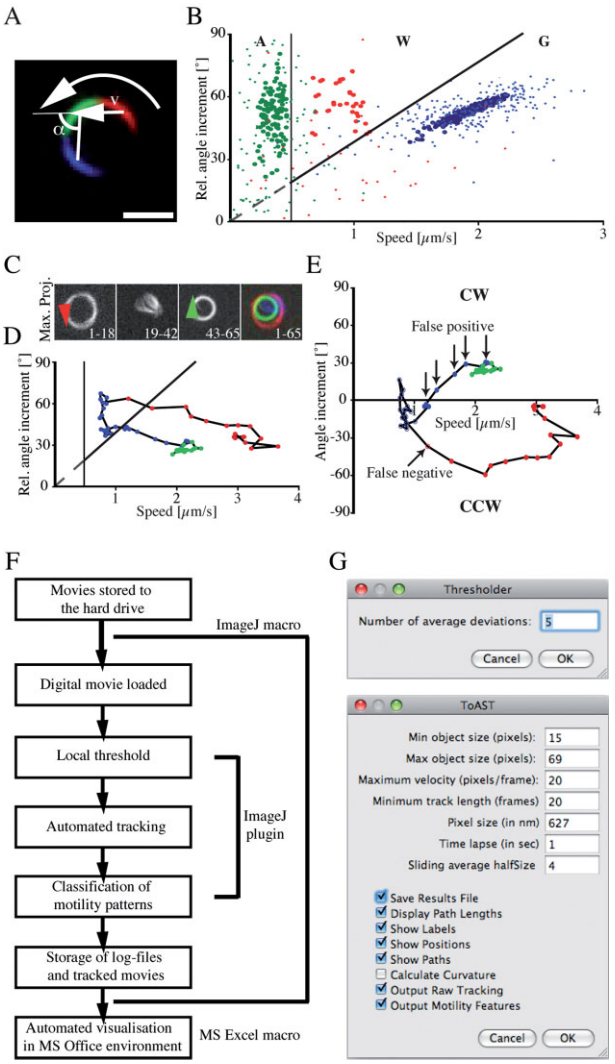

Figure 4. Principle of automated classification of sporozoite movement patterns. (A) A scheme representing digital calculation of speed v and angle α from three consecutive images. Scale bar = 10 μm. (B) Scatter plot of absolute values of the relative angle increment α plotted against speed v for sporozoites showing either attached (A, green), waving (W, red) or gliding (G, blue) pattern. Small dots display raw data points, while large dots represent averages over nine time points. Black lines indicate the separating thresholds: Attached parasites move slower than $v = 0.5$ μm/s (A, vertical line); gliding sporozoites show a strong correlation of α and v and are thus separated from wavers by an intersection line through the origin ($\alpha = 0.022\ v$). (C) Series of maximum intensity projections displaying a switching motility pattern of a sporozoite. The sporozoite glides in a wide CCW circle for 18 s (left panel, red arrow indicates direction of movement), waves for another 23 s (second panel) and glides CW, describing a small circle for 22 s (third panel, green arrow indicates direction of movement). The right projection represents a colored merge of the first three panels (red = CCW, blue = waving, green = CW). Numbers indicate time intervals in seconds. (D) *v versus* abs(α) scatter for the sporozoite described in (C). Subsequent data points that were averaged over nine time points are connected according to the color code from (C). (E) *v versus* α scatter for the sporozoite from (C) to distinguish directional gliding. Negative values correspond to CCW, positive values to CW motility. Values that were not assigned to gliding in (D) are not considered for classification, though they are still represented *via* empty circles. Arrows indicate false-negative CCW gliders (red circle) and false-positive wavers (filled blue circles). (F, G) Automated image analysis and data processing pipeline. (F) A scheme of consecutive steps with indication of the implementation level. (G) Command windows of the thresholding and main processing plugins for ImageJ with the parameters used for tracking sporozoites at 10× magnification.

rarely move when isolated from midguts [12], we next tested sporozoites isolated from mosquitoes at the same day from midguts, hemolymph and salivary glands. This confirmed the previous observations and showed that some sporozoites isolated from hemolymph moved by active gliding, while those in the salivary glands moved faster (Fig. 6E, F). When sporozoites were taken at early days (day 13) after infection and compared with sporozoites taken from the same infected batch of mosquitoes 6 days later, it was found that 20% of the day 13 sporozoites were gliding while at day 19 the proportion of movers increased to 50%. Concomitantly, the proportion of attached sporozoites decreased (Fig. 6G). This shows that ToAST is able to reveal differences between sporozoite populations and could in principle be useful for analyzing effects of different concentrations of drugs that inhibit motility. Indeed, investigating the actin dynamics-inhibiting drug cytochalasin D, which has long been known to inhibit apicomplexan parasite motility, rapidly confirmed that increasing drug concentrations decreased the number of sporozoites undergoing active gliding motility (Fig. 6H) [28].

4 Discussion

4.1 Towards automated tracking of *Plasmodium* sporozoites

We established a Tool for Automated Sporozoite Tracking (ToAST) that allows fully automated analysis of *Plasmodium* sporozoite movements. ToAST is based on the simple tracking of the speed and x-y position of a moving object from subsequent time frames with subsequent classification of the elementary steps of movement into four motility types. We developed ToAST for the purpose of tracking *Plasmodium berghei* sporozoites, which are simple crescent-shaped motile cells measuring about 12 μm in length and 1 μm across, and to distinguish their small set of simple movement patterns. Sporozoites are rather simple biological samples to track as they move mostly in circles. However, two other movement patterns ham-

A

Inexperienced users

Plugin \ %	Attached	Waving	Gliding
Attached	72	12	17
Waving	59	32	8
Gliding	49	8	43

Experienced users

Plugin \ %	Attached	Waving	Gliding
Attached	90	8	2
Waving	56	29	15
Gliding	37	6	58

B

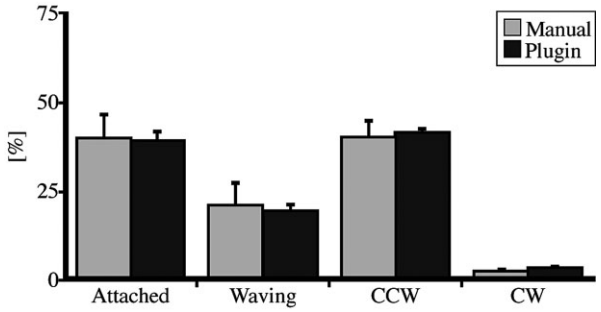

Figure 5. Reliability of ToAST *versus* manual classification. (A) The fit of classification of motility states for the 'difficult-to-classify' parasites from Fig. 3F by inexperienced and experienced users compared to the ToAST plugin. (B) Fit of the overall percentages of motility states for 100 parasites imaged over 100 s. The majority of sporozoites display a simple movement pattern. Note that the automated classification varies only little when using different thresholds (average threshold values with $n = 5, 7, 9$).

per analysis if one wants to image and automatically track dozens to hundreds of actively moving (gliding) sporozoites simultaneously. Furthermore, gliding sporozoites mainly glide in an apparent CCW fashion as observed under an inverted microscope, while only a small percentage (1–5%) move in the opposite direction [26]. We were able to separate the different movement types with high reliability by simply plotting the angle between subsequent displacements over the speed of the sporozoite. Depending on image acquisition parameters (frame rate, pixel size, binning), we needed to adjust the number of frames to average over nine time points before plotting the individual dots in a scatter plot (Fig. 4B). After adjusting these parameters, we achieved a high reliability in a standard sample when 100–250 sporozoites were imaged with a 10× lens. In such an image, a thresholded sporozoite consists of 40 ± 15 object pixels. The accuracy of the ToAST classification is highlighted by the different outcomes between individual observers, but also between different runs by a single observer, when errors in assigning patterns vary around the automatically established numbers (Fig. 5 and data not shown). In order to use ToAST, the fluorescent signal should be well over the background as a low signal-to-noise ratio will cause fluctuations in coordinate detection.

4.2 Towards high-throughput analysis

One of the motivations for developing ToAST was to generate a method for visual high-throughput screening to probe the effect of molecules (*e.g.* antibodies or chemicals) on apicomplexan parasite motility. As a proof of principle, we used ToAST to reveal differences in movement patterns and speed parameters of sporozoites isolated from mosquito salivary glands at different days post infection and at different temperatures. As sporozoites show similar distribution of movement patterns and a constant gliding speed over longer times when imaged at lower temperature, we would perform larger-scale analysis at 24°C rather than at 37°C. We also found that there was no detectable difference in the distribution of movement patterns between heavily infected and weakly infected salivary glands taken from mosquitoes at the same day post infection. However, differences between strongly and weakly infected mosquitoes might be revealed at different days post infection. Knowing from experience that mosquito infection underlies rather high variations, we propose two sets of alternative parameters potentially leading to the same output. For mosquitoes from cages with an average infection rate for our mosquito facility, we predict that it would be possible to image 40 wells of a 384-well plate each containing roughly 3000 sporozoites for 20 s, thus yielding information about movement parameters from around 10 000 filmed sporozoites within 1 h. In order to either compensate for a bad mosquito infection rate or to simply expand the number of conditions with a given amount of parasites, we suggest to alternatively use only 600 parasites per well (ca. 50 sporozoites in the field of view using a 10× objective) and film for 100 s. This procedure requires fewer mosquitoes per condition but provides a similar amount of data, although image acquisition will take five times longer. The former procedure will likely be preferable if we want to robustly distinguish effects on different movement patterns. This could indeed be important if performing small-scale screens of compounds targeted against, *e.g.*, different myosins, which we speculate could play distinct roles in the different parasite movements, or for examining different parasites.

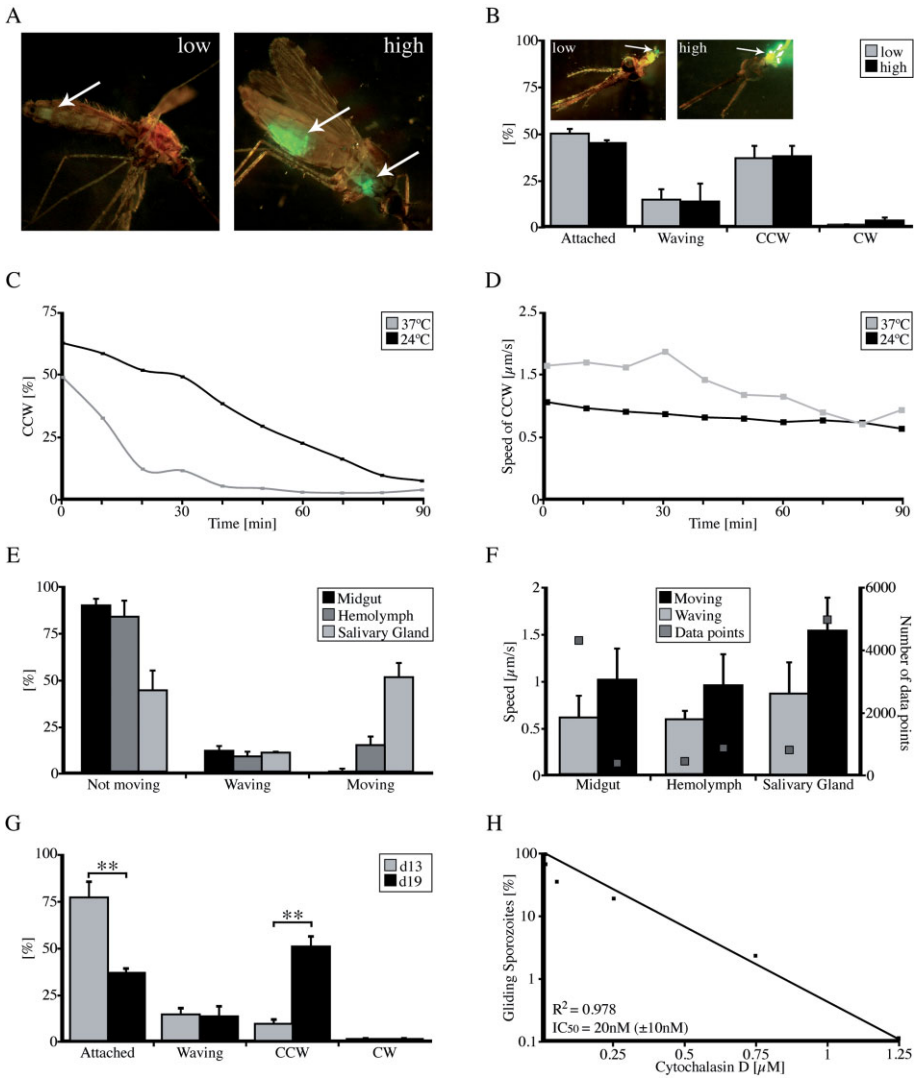

Figure 6. Sporozoite movement patterns and gliding speed vary with temperature, time, origin and age of the parasites. (A) Mosquitoes (22 days after infection) harboring GFP-expressing sporozoites display weak (left) and strong (right) levels of green fluorescence. Pictures were taken with identical exposure times. Salivary gland infection of the mosquito on the left could only be detected after dissection. (B) Quantitative analysis reveals that there is no difference in the motility pattern between parasites obtained from poorly (left inset) and highly (right inset) infected salivary glands. At this age of infection, the speed of the sporozoites was not significantly different (0.78 ± 0.04 μm/s *versus* 0.63 ± 0.1 μm/s for sporozoites from highly and poorly infected glands, respectively; $p = 0.11$). Insets show dissected heads with infected salivary glands still attached. Pictures were made using identical exposure times. Three highly and three poorly infected mosquitoes from the same age (22 days after infection) and cage were dissected, sporozoites were filmed and analyzed with ToAST using identical parameters. Average number of data points: 15 700 for highly infected glands, 9500 for low infected glands; the experiments were performed in triplicates. (C, D) Comparison of sporozoite CCW movement (C) and speed (D) at the indicated temperatures. At room temperature, the sporozoites describe a linear decrease in their rate of CCW movement (dropping rate: ca. 0.68%/min). An area with parasites was filmed for 100 s at 1 Hz every 10 min for a total of 90 min. (E) ToAST reveals differences in movement patterns according to their state of maturation. Immature sporozoites dissected from midguts show close to no effective movement (black bars). Parasites from the hemolymph show a pattern intermediate to those from midgut and salivary gland sporozoites. Error bars represent S.D. from three experiments. (F) Plot of the average speeds of parasites that were classified as either waving (light grey bars) or actively moving (black bars) in (E). Mature sporozoites (salivary glands) move and wave about 40–50% faster than those dissected from midguts and hemolymph ($p < 0.001$). Error bars represent S.D. from three experiments. The data points contributing to each average speed are plotted on the right *y* axis (grey boxes). (G) Differences in movement patterns of sporozoites isolated from salivary glands at different times after mosquito infection. Older sporozoites (19 days after infection, black bars) show a shifted pattern with mostly CCW gliding parasites. Asterisks indicate highly significant shifts in the respective pattern ($p < 0.01$). Experiments were performed using parasites of the same age from three independently bred and infected mosquito cages. Note the small standard deviation. (H) ToAST allows rapid evaluation of the effect of cytochalasin D on sporozoite gliding. All values represent the percentage of gliding parasites normalized to control parasites imaged in the absence of drug. The graph shows averages of triplicates from three different days using the following concentrations of cytochalasin D: 0, 0.05, 0.25, 0.75, and 1.25 μM. The number of gliding sporozoites decreases logarithmically under the influence of cytochalasin D (black trend line fits with $R^2 = 0.978$), leading to a complete inhibition of movement at 1.25 μM. The graph reveals an $IC_{50} = 20$ nM (±10 nM) for cytochalsin D in terms of inhibiting sporozoite gliding. Note that sporozoites gliding slower then 0.5 μm/s are not included in the analysis. For every condition, 11 000 data points in three independent experiments were analyzed.

In order to perform a full screen in a 384-well plate with 3000 sporozoites per well and 15 000 sporozoites isolated per mosquito, 80 infected mosquitoes would have to be dissected, which an experienced technician can achieve in 1 h. Note that some laboratories achieve salivary gland infection rates of up to 100 000 sporozoites per mosquito. Using a pipeting robot and an acquisition time of 20 s per movie, an entire 384-well plate could thus be tested under ideal conditions during one working day. To achieve this, sporozoites would not be added to the entire plate but in a row-by-row fashion after a single row is imaged. This is based on the observation that sporozoites move reliably for only about 45 min at 24°C. Movies are collected at the center of each well and stored to a hard drive. A single computer (2×2.66 GHz Dual-Core Intel Xenon, min. 2 GB RAM) would then take 6–9 h to extract the data and another hour for visualization of the complete data in Excel. Down-sampling of the images during acquisition could drop this time by about fourfold, if 2×2 bins are used, which still yielded reliable results (data not shown). Providing that enough insectary space and microscopy access is available, and taking into account the time to rear mosquitoes, infect with *P. berghei* or *P. yoelii,* dissect the salivary glands, fill the 384-well plate and evaluate the generated data, a single person should be able to test up to 1000 conditions (*i.e.* drugs) per week.

Lastly, our tracking and pattern classification tool is in principle readily adaptable to examine other motile stages of various parasites, such as *Plasmodium* ookinetes and *Toxoplasma* tachyzoites, or any other cell that moves in clearly distinguishable patterns, as the tracking tool solely rests on the plotting of the displacement angle over the speed. For the individual question or cell to be studied, however, parameters such as the number of frames recorded per second, the pixel size and number of the chip, the number of frames used for averaging speed or determining angular displacement have to be carefully tested and optimized. In conclusion, we provide a procedure to probe for inhibitors of sporozoite motility that adds a tool to those already existing for quantitative visual screening of infected liver cells [29–31] and the classical screens focused on infected red blood cells.

We thank Heiko Becher for advice and help on statistical analysis, Diana Scheppan for mosquito infection, Anne Dixius, Saskia Ziegler and our undergraduate students for manual annotation and tracking analysis, and Björn Alex, Marek Cyrklaff and Sylvia Münter for discussion and reading the manuscript. Our work is funded by grants from the Federal German Ministry for Education and Research (BMBF – BioFuture) and the German Research Foundation (DFG – SFB 544). Support from the Cluster of Excellence CellNetworks at the University of Heidelberg and the Institute of Computational Modelling at the Siberian Branch of the Russian Academy of Science is acknowledged. F.F. is an affiliated member of the European Network of Excellence BioMalPar. A.S. received a RISE fellowship from the German Academic Exchange Program (DAAD).

The authors have declared no conflict of interest.

5 References

[1] Young, G. M., Badger, J. L., Miller, V. L., Motility is required to initiate host cell invasion by *Yersinia enterocolitica*. *Infect. Immun.* 2000, *68*, 4323–4326.

[2] Tomich, M., Herfst, C. A., Golden, J. W., Mohr, C. D., Role of flagella in host cell invasion by *Burkholderia cepacia*. *Infect. Immun.* 2002, *70*, 1799–1806.

[3] O'Neil, H. S., Marquis, H., *Listeria monocytogenes* flagella are used for motility, not as adhesins, to increase host cell invasion. *Infect. Immun.* 2006, *74*, 6675–6681.

[4] Hill, K. L., Biology and mechanism of trypanosome cell motility. *Eukaryot. Cell* 2003, *2*, 200–208.

[5] Andrade, L. O., Andrews, N. W., The *Trypanosoma cruzi*-host-cell interplay: Location, invasion, retention. *Nat. Rev. Microbiol.* 2005, *3*, 819–823.

[6] Munter, S., Way, M., Frischknecht, F., Signaling during pathogen infection. *Sci. STKE* 2006, re5.

[7] Baum, J., Gilberger, T. W., Frischknecht, F., Meissner, M., Host-cell invasion by malaria parasites: Insights from *Plasmodium* and *Toxoplasma*. *Trends Parasitol.* 2008, *24*, 557–563.

[8] Schuler, H., Matuschewski, K., Regulation of apicomplexan microfilament dynamics by a minimal set of actin-binding proteins. *Traffic* 2006, *7*, 1433–1439.

[9] Schuler, H., Matuschewski, K., *Plasmodium* motility: Actin not actin' like actin. *Trends Parasitol.* 2006, *22*, 146–147.

[10] Cowman, A. F., Crabb, B. S., Invasion of red blood cells by malaria parasites. *Cell* 2006, *124*, 755–766.

[11] Vlachou, D., Schlegelmilch, T., Runn, E., Mendes, A., Kafatos, F. C., The developmental migration of *Plasmodium* in mosquitoes. *Curr. Opin. Genet. Dev.* 2006, *16*, 384–391.

[12] Matuschewski, K., Getting infectious: Formation and maturation of *Plasmodium sporozoites* in the *Anopheles* vector. *Cell. Microbiol.* 2006, *8*, 1547–1556.

[13] Vanderberg, J. P., Frevert, U., Intravital microscopy demonstrating antibody-mediated immobilisation of *Plasmodium berghei* sporozoites injected into skin by mosquitoes. *Int. J. Parasitol.* 2004, *34*, 991–996.

[14] Amino, R., Thiberge, S., Martin, B., Celli, S. *et al.*, Quantitative imaging of *Plasmodium* transmission from mosquito to mammal. *Nat. Med.* 2006, *12*, 220–224.

[15] Matsuoka, H., Yoshida, S., Hirai, M., Ishii, A., A rodent malaria, *Plasmodium berghei*, is experimentally transmitted to mice by merely probing of infective mosquito, *Anopheles stephensi*. *Parasitol. Int.* 2002, *51*, 17–23.

[16] Medica, D. L., Sinnis, P., Quantitative dynamics of *Plasmodium yoelii* sporozoite transmission by infected anopheline mosquitoes. *Infect. Immun.* 2005, *73*, 4363–4369.
[17] Yamauchi, L. M., Coppi, A., Snounou, G., Sinnis, P., *Plasmodium* sporozoites trickle out of the injection site. *Cell. Microbiol.* 2007, *9*, 1215–1222.
[18] Sidjanski, S., Vanderberg, J. P., Delayed migration of *Plasmodium* sporozoites from the mosquito bite site to the blood. *Am. J. Trop. Med. Hyg.* 1997, *57*, 426–429.
[19] Amino, R., Franke-Fayard, B., Janse, C., Waters, A. *et al.*, in: Shorte, S. L., Frischknecht, F. (Eds.), *Imaging Cellular and Molecular Biological Functions (Principle and Practice)*, Springer, Berlin 2007, pp. 345–360.
[20] Frischknecht, F., The skin as interface in the transmission of arthropod-borne pathogens. *Cell. Microbiol.* 2007, *9*, 1630–1640.
[21] Frischknecht, F., Baldacci, P., Martin, B., Zimmer, C. *et al.*, Imaging movement of malaria parasites during transmission by *Anopheles* mosquitoes. *Cell. Microbiol.* 2004, *6*, 687–694.
[22] Amino, R., Menard, R., Frischknecht, F., *In vivo* imaging of malaria parasites – recent advances and future directions. *Curr. Opin. Microbiol.* 2005, *8*, 407–414.
[23] Prudencio, M., Rodriguez, A., Mota, M. M., The silent path to thousands of merozoites: The *Plasmodium* liver stage. *Nat. Rev. Microbiol.* 2006, *4*, 849–856.
[24] Kappe, S. H., Buscaglia, C. A., Nussenzweig, V., *Plasmodium* sporozoite molecular cell biology. *Annu. Rev. Cell Dev. Biol.* 2004, *20*, 29–59.
[25] Yoeli, M., Movement of the sporozoites of *Plasmodium berghei* (Vincke et Lips, 1948). *Nature* 1964, *201*, 1344–1345.
[26] Vanderberg, J. P., Studies on the motility of *Plasmodium* sporozoites. *J. Protozool.* 1974, *21*, 527–537.
[27] Natarajan, R., Thathy, V., Mota, M. M., Hafalla, J. C. *et al.*, Fluorescent *Plasmodium berghei* sporozoites and pre-erythrocytic stages: A new tool to study mosquito and mammalian host interactions with malaria parasites. *Cell. Microbiol.* 2001, *3*, 371–379.
[28] Russell, D. G., Sinden, R. E., The role of the cytoskeleton in the motility of coccidian sporozoites. *J. Cell Sci.* 1981, *50*, 345–359.
[29] Prudencio, M., Rodrigues, C. D., Hannus, M., Martin, C. *et al.*, Kinome-wide RNAi screen implicates at least 5 host hepatocyte kinases in *Plasmodium* sporozoite infection. *PLoS Pathog.* 2008, *4*, e1000201.
[30] Cunha-Rodrigues, M., Prudencio, M., Mota, M. M., Haas, W., Antimalarial drugs – host targets (re)visited. *Biotechnol. J.* 2006, *1*, 321–332.
[31] Gego, A., Silvie, O., Franetich, J. F., Farhati, K. *et al.*, New approach for high-throughput screening of drug activity on *Plasmodium* liver stages. *Antimicrob. Agents Chemother.* 2006, *50*, 1586–1589.

